

Tomography scheme for two spin- $\frac{1}{2}$ qubits in a double quantum dot

Niklas Rohling and Guido Burkard

Department of Physics, University of Konstanz, D-78457 Konstanz, Germany

(Received 10 April 2013; published 2 August 2013)

We present a scheme for full quantum state tomography tailored for two spin qubits in a double quantum dot. A set of 15 quantum states allows to determine the density matrix in this two-qubit space by projective measurement. In this paper, we choose a set gained from mutually unbiased bases. We determine how those 15 projections can be represented by charge measurements after a spin-to-charge conversion and the application of quantum gates. The quantum gates include exchange-based gates as well as rotations by electron spin resonance (ESR). We assume the experimental realization of ESR operations to be more difficult than the exchange gate operation with respect to fidelity and speed. Therefore it is an important result that the ESR gates can be limited to a $\pi/2$ rotation for one of the electron spins per measurement.

DOI: [10.1103/PhysRevB.88.085402](https://doi.org/10.1103/PhysRevB.88.085402)

PACS number(s): 03.67.Lx, 03.65.Wj, 73.21.La, 85.75.-d

I. INTRODUCTION

Since electron spins in quantum dots were proposed¹ as qubits, a lot of experimental progress has been made with a two-electron double quantum dot as the basic cell of this kind of quantum computing; time evolution due to exchange interaction was demonstrated² as well as electron spin resonance (ESR) of one electron spin.³ Recently, Brunner and coworkers⁴ demonstrated both, exchange interaction and ESR rotation in the same double quantum dot. In principle, this allows to perform arbitrary quantum gates in this system. Ultimate control of a quantum system can be demonstrated in experiment by state tomography, i.e., gaining full information of a quantum state, in general described by a density matrix. Since the density matrix is Hermitian with trace 1, it can be described by $N^2 - 1$ real parameters for a N -dimensional Hilbert space. Therefore, from repeated projection of the unknown quantum state onto at least $N^2 - 1$ known states, the density matrix can be reconstructed from experimental data. A higher number of different measurements can increase the precision.⁵ The experimental values of measurements are not perfect due to external noise and because they are not performed infinitely often. This may lead to unphysical results for the estimation of the density matrix by violating the non-negativity condition. By applying maximum likelihood⁶⁻⁸ or Bayesian⁹⁻¹⁶ methods those results can be avoided.

State tomography was done in nuclear magnetic resonance experiments with qubits encoded by nuclear spins¹⁷ and is well established for experiments with trapped ions^{18,19} up to eight qubits.²⁰ It was also performed with superconducting qubits.^{21,22} For spin qubits, state tomography was done for qubits represented by the singlet and one triplet level of two electron spins in a double quantum dot for the single-qubit²³ and the two-qubit²⁴ cases as well as recently for an exchange-only qubit built by spin states of three electrons in a triple quantum dot.²⁵

Here, we present a measurement scheme for determining the unknown mixed quantum state of a two-qubit system realized by two electron spins in one double quantum dot. A complete set of measurements for the two-qubit space is, e.g., given by James *et al.*,⁷ in that case referred to the polarization of two photons. We use another series of projections, which is based on a set of so-called mutually unbiased bases²⁶⁻²⁹ and

which includes entangled states in contrast to Ref. 7. In this issue, our scheme also differs from the scheme used in Ref. 24 where the state of each of the two qubits, both encoded in one two-electron double quantum dot, is measured separately and the density matrix is determined using correlation data. The measurements we propose are projections on one-dimensional subspaces of the four-dimensional Hilbert space and thus joint measurements on the full two-qubit space. An important result of our paper is that these measurements can be done by applying ESR maximally for a $\pi/2$ rotation on one of the electron spins per measurement. There are two reasons why an experimentalist may want to avoid long ESR-based rotations. First, ESR rotations are slower than exchange-based gates. According to Ref. 30, the shortest operation times realized for an ESR π rotation are 20 ns³¹ for lateral quantum dots and 8.5 ns^{32,33} for quantum dots in nanowires whereas the shortest time for an exchange-based SWAP gate is 0.35 ns.² In the experiment of Ref. 4, where both ESR and exchange interaction are realized, the time for a complete ESR π rotation was around 400 ns, whereas an exchange-based SWAP gate was achieved within 10 ns. Second, we assume the ESR gates to have a lower fidelity than exchange gates.

In Sec. II, we describe the double-dot system with two electrons and the possible manipulation of the quantum states. Section III provides information on the matrix space for the traceless part of two-qubit density matrices and on properties of a basis in this space represented by pure quantum states. The main result of this paper, a scheme for constructing such a set of quantum states using quantum gates and spin-to-charge conversion, is given in Sec. IV. In Sec. V, we discuss how the influence of imperfection in the quantum gates might be treated in experiment, before we conclude in Sec. VI.

II. PHYSICAL SYSTEM

We consider a double quantum dot with two electrons taking only the lowest (orbital) energy level in each dot into account. Therefore, due to the antisymmetry of the wave function (Pauli principle), we have a six-dimensional Hilbert space since we have one state with both electrons in the left dot, one state with two electrons in the right dot, and a four-dimensional space with one electron per dot. We will denote charge states with n_l electron in the left and n_r electrons in the right dot with

(n_l, n_r) . The Hamiltonian, taking into account the difference between the energy levels, ε , the Coulomb penalty for both electrons in the same dot, U , and the hopping matrix element between the dots, t , reads

$$H = \frac{\varepsilon}{2}(\hat{n}_1 - \hat{n}_2) + \frac{U}{2} \sum_{i=1,2} \hat{n}_i(\hat{n}_i - 1) + t \sum_{s=\uparrow,\downarrow} (\hat{c}_{2s}^\dagger \hat{c}_{1s} + \hat{c}_{1s}^\dagger \hat{c}_{2s}), \quad (1)$$

where the operators of the occupation number in the dots, \hat{n}_1 and \hat{n}_2 are given by $\hat{n}_i = \sum_{s=\uparrow,\downarrow} \hat{c}_{is}^\dagger \hat{c}_{is}$.

We will consider the states with charge configuration (1,1) as logical Hilbert space and regard the electron spin in each dot as a quantum bit. The aim of this paper is to give a scheme for determining an unknown density matrix of this two-qubit space. In the limit $|t| \ll |U \pm \varepsilon|$, the (1,1) states are approximately decoupled from the states with charge configuration (2,0) and (0,2). For this case, the effective Hamiltonian for (1,1) states can be obtained by applying a Schrieffer-Wolff transformation,³⁴

$$H_{\text{eff}} = J \frac{\sigma_1 \cdot \sigma_2 - 1}{4} = -J P_S \quad (2)$$

with $J = 4t^2U/(U^2 - \varepsilon^2)$, and where σ_i is the vector of Pauli matrices for the electron spin in dot $i = 1, 2$. Note that H_{eff} is given by $-J$ times the projection operator P_S on the spin singlet $|S\rangle = \frac{|\uparrow\downarrow\rangle - |\downarrow\uparrow\rangle}{\sqrt{2}}$ because only an antisymmetric state can couple to the (0,2) and to the (2,0) space. The strength of this exchange coupling, J , can be tuned in experiment by varying ε or t .

We now consider in addition to the exchange interaction above a magnetic field yielding the Zeeman Hamiltonian

$$H_B = \mathbf{h}_1 \cdot \sigma_1 + \mathbf{h}_2 \cdot \sigma_2. \quad (3)$$

Let us restrict the discussion first to a magnetic field only in z direction, $\mathbf{h}_1 = h_{1z}\mathbf{e}_z$, $\mathbf{h}_2 = h_{2z}\mathbf{e}_z$. The homogeneous part of the magnetic field, $h_z = \frac{h_{1z} + h_{2z}}{2}$, splits off the triplet states, because $|T_+\rangle = |\uparrow\uparrow\rangle$ and $|T_-\rangle = |\downarrow\downarrow\rangle$ obtain the Zeeman energy $\pm 2h_z$, whereas $|T_0\rangle = \frac{|\uparrow\downarrow\rangle + |\downarrow\uparrow\rangle}{\sqrt{2}}$ is not affected. A gradient in the magnetic field, described by $\Delta h_z = h_{1z} - h_{2z}$, leads to a mixing of $|S\rangle$ and $|T_0\rangle$. If $|\Delta h_z|$ and $|h_z|$ are large compared to $4t^2/U$, which is the value of J for $\varepsilon = 0$, then the energy eigenstates with charge configuration (1,1) are approximately $|T_+\rangle, |T_-\rangle, |\uparrow\downarrow\rangle, |\downarrow\uparrow\rangle$. At higher values of ε , $|S\rangle$ becomes an energy eigenstate, see Fig. 1. Different directions in the magnetic field in the left and the right quantum dots can additionally induce an avoided crossing between $|\uparrow\uparrow\rangle$ and $|S\rangle$.

Projective measurements on the two-qubit space are done by charge measurements after a spin-to-charge conversion,^{35,36} which we describe in the following. For $\varepsilon = 0$, the four lowest energy levels belong to states with charge configuration (1,1), which constitute the logical subspace of the system. The starting point is an arbitrary state $|\psi\rangle$ in this logical subspace and $\varepsilon = 0$. By changing gate voltages, ε can be increased to a value higher than U , modifying the spectrum to a situation where the state (0,2) is the ground state of the system, see Fig. 1(a). Performing this varying of ε backwards in time would map the (0,2) charge state on one specific state in the

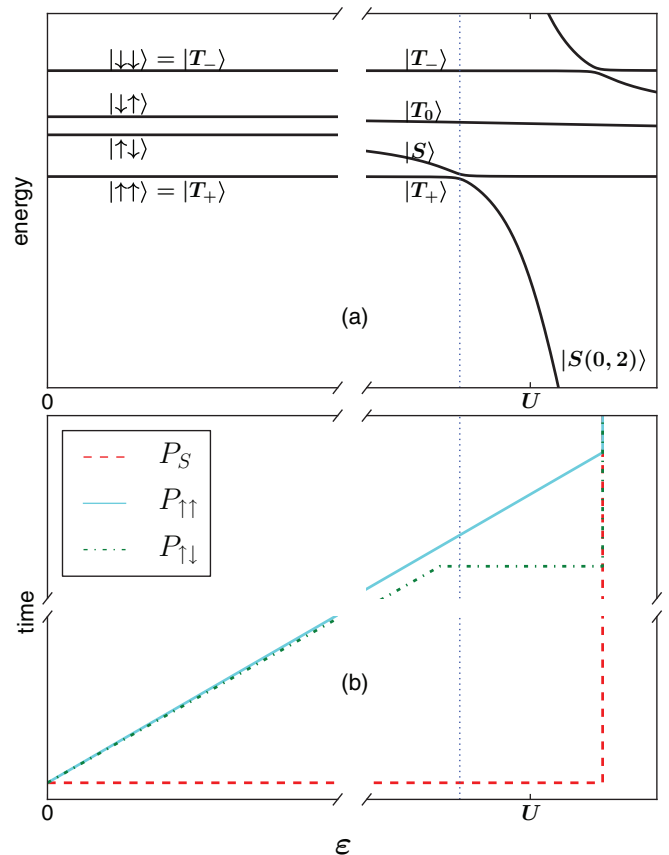


FIG. 1. (Color online) (a) Spectrum of a two-electron double quantum dot with a magnetic field with $|h_z| \gg |\Delta h_z| \gg 4t^2/U$, $h_z, \Delta h_z < 0$ for small values of ε and ε close to U . The avoided crossing between $|S\rangle$ and $|\uparrow\uparrow\rangle$ at the blue dotted line is induced by slightly different directions of the magnetic fields in the left and the right dot. (b) Three ways to tune ε to achieve projection on $|\uparrow\downarrow\rangle$, dash-dotted (green) line, on $|S\rangle$, dashed (red) line, and on $|\uparrow\uparrow\rangle$, solid (cyan) line. Note that the ε axis and the time axis are broken.

logical subspace, $|\psi_s\rangle$. The forward procedure thus converts the $|\psi_s\rangle$ amount of $|\psi\rangle$, given by $\langle\psi_s|\psi\rangle|\psi_s\rangle$, to the (0,2) charge state and the remaining contributions of $|\psi\rangle$ are still in charge configuration (1,1). Therefore, measuring a charge state (0,2), corresponds to a projection onto the state $|\psi_s\rangle$ in the logical subspace. Now, we will consider three different cases shown in Fig. 1(b) and explain which is the state $|\psi_s\rangle$ for the different time dependencies of ε . Assuming we are in the situation shown in Fig. 1(a), then a slow change of ε from 0 to a value higher than U would be an adiabatic transition of the $|T_+\rangle$ state to the (0,2) state. If we increase ε slowly from 0 up to a value below the avoided crossing between $|S\rangle$ and $|T_+\rangle$ and then proceed fast through this avoided crossing, the charge readout effectively projects onto the state $|\uparrow\downarrow\rangle$. An overall fast transition yields a projection onto $|S\rangle$. We will use this three different kinds of projection in our scheme for state tomography in Sec. IV. In the state-tomography experiment for the $S - T_0$ qubits^{23,24} the projections onto $|\uparrow\downarrow\rangle$ and onto $|S\rangle$ were used. To allow projections onto other than the three states described so far, we assume quantum gates to be applied prior to the sweep. In principle, more complicated transitions are possible and they are described

by a Landau-Zener transition.^{37,38} State preparation is done in the opposite direction by converting the (0,2) state in a well-defined (1,1) charge state.

It has been shown that the exchange interaction together with arbitrary single-qubit rotations allows for universal quantum computing,¹ i.e., every unitary operation can be constructed from these elementary gates. To achieve full control on a single qubit, a tunable magnetic field in one direction is necessary with individual tuning for each dot. We assume the magnetic field to point in z direction. Therefore the vector on the Bloch sphere, which represents the qubit state, performs a rotation around the z axis. The individual tuning of the magnetic fields in both dots (field gradient) together with control over the pulse times thus allows for controlling one angle on the Bloch sphere of each spin. Additionally, rotations on the Bloch sphere around another axis than the z axis are required, which can be done using ESR. This requires an oscillating magnetic field orthogonal to the axis of the time-independent magnetic field. For a single qubit in resonance, the Hamiltonian is given by $H_{\text{ESR}} = h_z \sigma_z + h_x \cos(2h_z t) \sigma_x$. The frequency of the oscillation is the Larmor frequency h_z of the constant field. For $h_x \ll h_z$, the corresponding Schrödinger equation can be solved approximately by using a rotating wave approximation. Then the result reads $|\psi(t)\rangle = e^{ih_z t \sigma_z} e^{ih_x t / 2 \sigma_x} |\psi(0)\rangle$. By going from the laboratory frame to a rotating frame with frequency $2h_z$ around the z axis, an ESR pulse can be expressed as a mere rotation around one axis, see Appendix D. However, this does not completely resolve the issue of the required control over the pulse times as introduced above as control over the z rotation. The first reason is that a phase shift in the ESR oscillation, $\cos(2h_z t) \rightarrow \cos(2h_z t + \phi_{\text{shift}})$ can occur randomly, when the pulse times are not controlled, and this can change the axis of the ESR rotation. Second, the gradient between the magnetic field in the left and the right dots requires control as the frame of reference is the same for both qubits. The frequency of the rotation around the x axis is determined by the amplitude of the oscillating magnetic field in x direction. As quantum gates are desired to be fast, the value of h_x is supposed to be as large as possible. While a strong high-frequency magnetic field is hard to realize experimentally, Brunner *et al.*⁴ used an inhomogeneous magnetic field and achieved an effective time dependence in the Zeeman Hamiltonian by applying an ac voltage shifting the electron back and forth. Due to an offset in Zeeman energy between the dots, it was possible to perform ESR on each of the dots separately. Since exchange interaction was performed as well, in this double dot sample, operations allowing for full control on the two-qubit space have been demonstrated experimentally.

III. GENERAL CONSIDERATIONS ABOUT TWO-QUBIT TOMOGRAPHY

We want to find a scheme for state tomography for the two-qubit space. This means the scheme has to provide the full information of the density matrix ρ , which is a Hermitian 4×4 matrix with trace 1. Therefore we need at least 15 different measurements to determine the 15 real parameters describing ρ . In the space of 4×4 matrices, we can introduce the scalar product $\langle A|B \rangle_M := \text{tr}(A^\dagger B)$ and the basis

$\{D_k = \frac{\sigma_{1i}\sigma_{2j}}{2}$ with $k = 4i + j$ and $i, j \in \{0, x \equiv 1, y \equiv 2, z \equiv 3\}$ where $\sigma_{1j} := \sigma_j \otimes \mathbb{1}$ and $\sigma_{2j} := \mathbb{1} \otimes \sigma_j$ are Pauli matrices for the first or second spin, and $\sigma_{n0} = \mathbb{1}$. Note that this basis is orthonormal with respect to $\langle \cdot | \cdot \rangle_M$ because $\langle \sigma_{1i}\sigma_{2j} | \sigma_{1k}\sigma_{2l} \rangle_M = 4\delta_{ik}\delta_{jl}$. We can expand ρ in the $\{D_k\}$ basis,

$$\rho = \sum_{k=0}^{15} \rho_k D_k. \quad (4)$$

We know already that all ρ_k are real because ρ is Hermitian and that $\rho_0 = 1/2$ due to the trace condition. The aim of the tomography is to determine every parameter $\rho_k, k = 1, \dots, 15$.

Estimations for ρ_1, \dots, ρ_{15} have to be acquired from experimental data. In the physical setup, we consider in this paper, measurements are done by measuring the charge state after increasing the detuning ε . This converts a state from the logical spin space (qubit space) with charge configuration (1,1) to a (0,2) charge state. In the previous section we found conditions under which this leads to a projective measurement on either $|\uparrow\downarrow\rangle$, $|S\rangle$, or $|T_+\rangle$. We assume that universal quantum gates are feasible and, therefore, any other state could have been mapped by a unitary operation onto the state that is converted to the (0,2) charge state. Therefore spin-to-charge conversion and universal quantum gates allow for a projection onto an arbitrary state $|\phi\rangle$. Each measurement within the tomography scheme will project onto a state $|\phi_j\rangle$ and thus yields $\text{tr}(|\phi_j\rangle\langle\phi_j|\rho)$. The projection operator $P_j = |\phi_j\rangle\langle\phi_j|$ is also a Hermitian 4×4 matrix with trace 1, which means $\langle P_j | D_0 \rangle_M = \frac{1}{2} \langle P_j | \mathbb{1} \rangle_M = 1/2$. Nevertheless, P_j can be expressed in terms of the six real parameters⁴⁵ for the state $|\phi_j\rangle$. For P_j given in the $\frac{\sigma_{1i}\sigma_{2j}}{2}$ basis, see Appendix A. We are seeking a set $\{|\phi_j\rangle\}$ that provides full information of ρ . If 15 projectors fulfill the condition that $\{P_j - \mathbb{1}/4, j=1, \dots, 15\}$ is a basis in the space of traceless 4×4 matrices, we call these projectors a minimal set or quorum.

We introduce the invertible 15×15 matrix \mathcal{P} with

$$\mathcal{P}_{jk} = \langle P_j | D_k \rangle_M \quad \text{with } j, k = 1, \dots, 15, \quad (5)$$

i.e., considering only the traceless contributions of the projectors P_j . Since $\text{tr}(P_j \rho) = \frac{1}{4} + \sum_{k=1}^{15} \mathcal{P}_{jk} \rho_k$, the parameters ρ_k are given by $\rho_k = \sum_{j=1}^{15} \mathcal{P}_{kj}^{-1} (\text{tr}(P_j \rho) - \frac{1}{4})$. We obtain an experimental estimation m_j for $\text{tr}(P_j \rho)$ by dividing the number of the charge state (0,2) outcomes by the number of experimental runs for the j th projection experiment. This statistical data does not yield the exact values of ρ_k but estimations for it, which we call $\tilde{\rho}_k$ and which are by linear reconstruction given by

$$\begin{pmatrix} \tilde{\rho}_1 \\ \vdots \\ \tilde{\rho}_{15} \end{pmatrix} = \mathcal{P}^{-1} \begin{pmatrix} m_1 - \frac{1}{4} \\ \vdots \\ m_{15} - \frac{1}{4} \end{pmatrix}. \quad (6)$$

Although the maximum likelihood method would be preferred over the linear reconstruction for practical purposes we want to consider Eq. (6) in order to obtain information about the influence of \mathcal{P} on the statistical error expressed by the covariance matrix $C_{kl} = E[(\tilde{\rho}_l - \rho_l)(\tilde{\rho}_k - \rho_k)]$ where $E(\cdot)$ is the expectation value of the probability distribution, which is given by the density matrix ρ and the set of measurements

P_1, \dots, P_{15} . Note that $E(\cdot)$ is in general not expressed by the quantum mechanical expectation value $\text{tr}(O\rho)$ of an operator O , but this is the case for those operators which are directly measured, i.e., for every $j = 1, \dots, 15$ we have a binomial distribution with the number of trials, N_j , and the probability of success $\text{tr}(P_j\rho)$. The probability distribution for the indirectly obtained stochastic variables $\tilde{\rho}_k$ has to be gained using the matrix \mathcal{P} . Using Eq. (6), we find for the covariance matrix

$$C_{kl} = E \left\{ \sum_{j=1}^{15} \mathcal{P}_{kj}^{-1} [m_j - \text{tr}(P_j\rho)] \sum_{i=1}^{15} [m_i - \text{tr}(P_i\rho)] \mathcal{P}_{li}^{-1} \right\} \\ = \sum_{i,j=1}^{15} \mathcal{P}_{kj}^{-1} \underbrace{E\{[(m_j - \text{tr}(P_j\rho))][m_i - \text{tr}(P_i\rho)]\}}_{=B_{ji}} \mathcal{P}_{li}^{-1}, \quad (7)$$

which is equivalent to $C = \mathcal{P}^{-1}B(\mathcal{P}^{-1})^T$. Our aim is to find a set of measurement for which every value $|C_{kl}|$ is small. The covariance matrix of the measurement results, B , is given by $B_{ji} = \delta_{ji} \text{tr}(P_j\rho)[1 - \text{tr}(P_j\rho)]/N_j \leq \delta_{ji}/(4N_j)$ as a property of the binomial distribution describing m_j , and the upper limit is reached if $\text{tr}(P_j\rho) = 1/2$. Using the adjugate matrix, $(\text{adj } \mathcal{P})_{kl} = (-1)^{k+l} \det(\mathcal{P}_{/l/k})$, where $\mathcal{P}_{/l/k}$ is the matrix one gains by deleting the l th row and the k th column of \mathcal{P} , to express the inverse of \mathcal{P} , we obtain

$$|C_{kl}| = \left| \sum_{j=1}^{15} \mathcal{P}_{kj}^{-1} \mathcal{P}_{lj}^{-1} \frac{\text{tr}(P_j\rho)[1 - \text{tr}(P_j\rho)]}{N_j} \right| \\ \leq \sum_{j=1}^{15} \frac{|(\text{adj } \mathcal{P})_{kj}(\text{adj } \mathcal{P})_{lj}|}{4N_j \det(\mathcal{P})^2}. \quad (8)$$

The length in matrix space of $P_j - \mathbb{1}/4$, i.e., a row of \mathcal{P} , is $\sqrt{\langle P_j - \mathbb{1}/4 | P_j - \mathbb{1}/4 \rangle_M} = \sqrt{\frac{3}{4}}$. A determinant is invariant under the Gram-Schmidt orthogonalization, yielding upper limits for $|\det(\mathcal{P})|$ as well as for the matrix elements of the adjugate matrix of \mathcal{P} , which are determinants of 14×14 matrices gained from \mathcal{P} by deleting one row and one column. For $\text{adj } \mathcal{P}$ we find $|(\text{adj } \mathcal{P})_{kj}| \leq (\frac{3}{4})^{\frac{14}{2}}$. Assuming $N_1 = N_2 = \dots = N_{15} = N$, this results in the following inequality:

$$|C_{kl}| \leq \frac{15(\frac{3}{4})^{14}}{4N \det(\mathcal{P})^2} \approx \frac{0.06682}{N \det(\mathcal{P})^2}. \quad (9)$$

We now concentrate on maximizing the value $\det(\mathcal{P})^2$. The upper bound for $|\det(\mathcal{P})|$ is given by $(\frac{3}{4})^{\frac{15}{2}} \approx 0.1156$, which would be reached if the rows of \mathcal{P} were orthogonal, which means the 15 projectors P_j have to fulfill

$$\langle P_j - \mathbb{1}/4 | P_k - \mathbb{1}/4 \rangle_M = 0 \Leftrightarrow \langle P_j | P_k \rangle_M = |\langle \phi_j | \phi_k \rangle|^2 \\ = 1/4 \quad \text{for } j \neq k. \quad (10)$$

In Appendix B, we prove that this is not possible.

The quorum from Ref. 7 for the two-qubit space, after translation from photon polarization states to spin states, reads $\{|\uparrow\uparrow\rangle, |\uparrow\downarrow\rangle, |\downarrow\uparrow\rangle, |\downarrow\downarrow\rangle, |\downarrow_y\uparrow\rangle, |\downarrow_y\downarrow\rangle, |\uparrow_x\downarrow\rangle, |\uparrow_x\uparrow\rangle, |\uparrow_x\downarrow_y\rangle, |\uparrow_x\uparrow_x\rangle, |\downarrow_y\uparrow_x\rangle, |\uparrow\uparrow_x\rangle, |\downarrow\uparrow_x\rangle, |\downarrow\uparrow_y\rangle, |\uparrow\uparrow_y\rangle, |\downarrow_y\uparrow_y\rangle\}$, where $|\uparrow_y\rangle = \frac{|\uparrow\rangle+i|\downarrow\rangle}{\sqrt{2}}$, $|\downarrow_y\rangle = \frac{|\uparrow\rangle-i|\downarrow\rangle}{\sqrt{2}}$, and $|\uparrow_x\rangle = \frac{|\uparrow\rangle+|\downarrow\rangle}{\sqrt{2}}$. We have removed the state $|\downarrow\downarrow\rangle$ because 15 states are sufficient here. These basis states are all separable and lead to $|\det(\mathcal{P})| = \frac{1}{5^{12}} \approx 2 \times 10^{-3}$.

A better result can be obtained by the well-known concept of mutually unbiased bases.^{26,29} Two bases in Hilbert space are called mutually unbiased if a state of the first basis has the same overlap with all states of the second basis. The idea of mutually unbiased bases originally referred to a situation where $N + 1$ observables in an N -dimensional Hilbert space are measured,²⁶ and each of these measurements yields, in the non-degenerate case, the probabilities for being in the corresponding N eigenstates, which are here chosen to be basis states of one of the mutually unbiased bases. In that case, it was shown that the mutually unbiased bases represent an optimal set to determine ρ in the sense of minimizing the statistical error.²⁷ For the projective measurement by the spin-to-charge conversion, which we consider in this paper, the situation is slightly different since every projection is done by another measurement. In particular, it is not necessary to measure all 20 probabilities; it suffices to perform the projective measurement for three states out of the four states in each of the five bases, providing a basis in the 15 dimensional matrix space, and consequently a minimal set of projectors. It has been shown that for a N -level system a set of $N + 1$ mutually unbiased bases exist if N is the integer power of a prime number.²⁷ Hence, for our four-dimensional case, five bases $\{|\phi_{0,1}\rangle, |\phi_{0,2}\rangle, |\phi_{0,3}\rangle, |\phi_{0,4}\rangle, \dots, \{|\phi_{4,1}\rangle, \dots, |\phi_{4,4}\rangle\}$ fulfilling

$$|\langle \phi_{jk} | \phi_{lm} \rangle|^2 = \delta_{jl}\delta_{km} + \frac{1 - \delta_{jl}}{4} \quad (11)$$

can be found. Note that states from different bases with numbers $j \neq l$ fulfill $|\langle \phi_{jk} | \phi_{lm} \rangle|^2 = \frac{1}{4}$, which is the condition (10). This means that the matrix space spanned by the traceless parts of the corresponding projectors contains five three-dimensional orthogonal subspaces. On the other hand, the states in the same basis are orthogonal in Hilbert space, $\langle \phi_{jk} | \phi_{jm} \rangle = \delta_{mk}$. We show in Appendix C that this always leads to $|\det(\mathcal{P})| = \frac{1}{32} = 0.03125$.

IV. EXPLICIT CONSTRUCTION OF SPIN-QUBIT QUORUM

We use a set of mutually unbiased bases given in Ref. 28 and present an explicit construction of the following 15 states out of these bases, forming a quorum,

$$|\psi_1\rangle = |\uparrow\uparrow\rangle, \quad P_1 = \frac{\mathbb{1} + \sigma_{1z} + \sigma_{2z} + \sigma_{1z}\sigma_{2z}}{4}, \\ |\psi_2\rangle = |\uparrow\downarrow\rangle, \quad P_2 = \frac{\mathbb{1} + \sigma_{1z} - \sigma_{2z} - \sigma_{1z}\sigma_{2z}}{4}, \\ |\psi_3\rangle = \text{SWAP}|\uparrow\downarrow\rangle = |\downarrow\uparrow\rangle, \quad P_3 = \frac{\mathbb{1} - \sigma_{1z} + \sigma_{2z} - \sigma_{1z}\sigma_{2z}}{4},$$

$$\begin{aligned}
|\psi_4\rangle &= e^{i\frac{\pi}{2}\sigma_{2z}}\sqrt{\text{SWAP}}e^{i\frac{\pi}{4}\sigma_{1x}}|S\rangle = |\uparrow_x\uparrow_x\rangle, & P_4 &= \frac{\mathbb{1} + \sigma_{1x} + \sigma_{2x} + \sigma_{1x}\sigma_{2x}}{4}, \\
|\psi_5\rangle &= e^{i\frac{\pi}{2}\sigma_{1z}}|\psi_4\rangle = |\downarrow_x\uparrow_x\rangle, & P_5 &= \frac{\mathbb{1} - \sigma_{1x} + \sigma_{2x} - \sigma_{1x}\sigma_{2x}}{4}, \\
|\psi_6\rangle &= e^{i\frac{\pi}{2}\sigma_{2z}}|\psi_4\rangle = |\uparrow_x\downarrow_x\rangle, & P_6 &= \frac{\mathbb{1} + \sigma_{1x} - \sigma_{2x} - \sigma_{1x}\sigma_{2x}}{4}, \\
|\psi_7\rangle &= e^{-i\frac{\pi}{4}(\sigma_{1z} + \sigma_{2z})}|\psi_4\rangle = |\uparrow_y\uparrow_y\rangle, & P_7 &= \frac{\mathbb{1} + \sigma_{1y} + \sigma_{2y} + \sigma_{1y}\sigma_{2y}}{4}, \\
|\psi_8\rangle &= e^{i\frac{\pi}{2}\sigma_{1z}}|\psi_7\rangle = |\downarrow_y\uparrow_y\rangle, & P_8 &= \frac{\mathbb{1} - \sigma_{1y} + \sigma_{2y} - \sigma_{1y}\sigma_{2y}}{4}, \\
|\psi_9\rangle &= e^{i\frac{\pi}{2}\sigma_{2z}}|\psi_7\rangle = |\uparrow_y\downarrow_y\rangle, & P_9 &= \frac{\mathbb{1} + \sigma_{1y} - \sigma_{2y} - \sigma_{1y}\sigma_{2y}}{4}, \\
|\psi_{10}\rangle &= e^{i\frac{\pi}{4}\sigma_{1x}}e^{i\frac{\pi}{8}(\sigma_{1z} - \sigma_{2z})}|S\rangle, & P_{10} &= \frac{\mathbb{1} - \sigma_{1z}\sigma_{2x} - \sigma_{1x}\sigma_{2y} - \sigma_{1y}\sigma_{2z}}{4}, \\
|\psi_{11}\rangle &= e^{i\frac{\pi}{2}\sigma_{1z}}|\psi_{10}\rangle, & P_{11} &= \frac{\mathbb{1} - \sigma_{1z}\sigma_{2x} + \sigma_{1x}\sigma_{2y} + \sigma_{1y}\sigma_{2z}}{4}, \\
|\psi_{12}\rangle &= e^{i\frac{\pi}{2}\sigma_{2z}}|\psi_{10}\rangle, & P_{12} &= \frac{\mathbb{1} + \sigma_{1z}\sigma_{2x} + \sigma_{1x}\sigma_{2y} - \sigma_{1y}\sigma_{2z}}{4}, \\
|\psi_{13}\rangle &= e^{-i\frac{\pi}{4}(\sigma_{1z} + \sigma_{2z})}|\psi_{10}\rangle, & P_{13} &= \frac{\mathbb{1} + \sigma_{1y}\sigma_{2x} - \sigma_{1z}\sigma_{2y} + \sigma_{1x}\sigma_{2z}}{4}, \\
|\psi_{14}\rangle &= e^{i\frac{\pi}{2}\sigma_{1z}}|\psi_{13}\rangle, & P_{14} &= \frac{\mathbb{1} - \sigma_{1y}\sigma_{2x} - \sigma_{1z}\sigma_{2y} - \sigma_{1x}\sigma_{2z}}{4}, \\
|\psi_{15}\rangle &= e^{i\frac{\pi}{2}\sigma_{2z}}|\psi_{13}\rangle, & P_{15} &= \frac{\mathbb{1} - \sigma_{1y}\sigma_{2x} + \sigma_{1z}\sigma_{2y} + \sigma_{1x}\sigma_{2z}}{4}, \tag{12}
\end{aligned}$$

where the states $|\psi_{3i+1}\rangle, |\psi_{3i+2}\rangle, |\psi_{3i+3}\rangle$ are belonging to the same basis, $i = 0, 1, 2, 3, 4$. The first three bases ($i = 0, 1, 2$) are given by the product of spin states in each dot where the quantization axis is chosen to be z , x , and y , thus those states are separable. The other two bases ($i = 3, 4$) consist of maximally entangled states.

Within the scheme we are using projective measurements on the states $|\uparrow\uparrow\rangle$, $|\uparrow\downarrow\rangle$, and $|S\rangle$ as described in Sec. II. In order to access the states in the set above not directly given by one of these states, we apply various quantum gates directly available for spin qubits, see Fig. 2. The SWAP gate is defined by $\text{SWAP}|s_1s_2\rangle = |s_2s_1\rangle$, i.e., it interchanges the information of the first and the second qubit. It can be realized by applying the exchange interaction (2) for a time t_e given by $\varphi = \int_0^{t_e} J(\tau)d\tau = \pi$, where we neglected the magnetic field (gradient) which is possible if J is large compared to $|\Delta h_z|$. Consequently, the $\sqrt{\text{SWAP}}$ gate can be achieved by applying the exchange interaction for yielding $\varphi = \pi/2$.

Since $\sigma_{1z} + \sigma_{2z}$ commutes with the exchange coupling, the influence of h_z can be treated formally as if it was applied before or after the exchange interaction. Furthermore, we need an ESR pulse on the first spin to access the states $|\psi_4\rangle, \dots, |\psi_{15}\rangle$. We want to emphasize that for each of these twelve states we need only one ESR $\pi/2$ rotation, $e^{i\frac{\pi}{4}\sigma_{1x}}$ of only one of the spins. As we assume the fidelity of ESR operations to be lower than that of exchange gates or rotations around the z axis, this is a crucial point for an experimental realization of a tomography scheme in a double quantum dot.

Note that ESR cannot be completely avoided because exchange interaction and rotations due to a static magnetic field together with the projections on $|\uparrow\downarrow\rangle, |S\rangle, |\uparrow\uparrow\rangle$ can only access the five-dimensional subspace in matrix space spanned by $\{\sigma_{1z}, \sigma_{2z}, \sigma_{1z}\sigma_{2z}, \sigma_{1x}\sigma_{2x} + \sigma_{1y}\sigma_{2y}, \sigma_{1x}\sigma_{2y} - \sigma_{1y}\sigma_{2x}\}$. This can be seen by regarding the time evolution under exchange interaction, which leaves $P_{\uparrow\uparrow} = P_1$ and P_S invariant and evolves $P_{\uparrow\downarrow} = P_2$ to

$$e^{i\varphi P_S} P_{\uparrow\downarrow} e^{-i\varphi P_S} = \frac{\mathbb{1} + \sigma_{1z}\sigma_{2z} + \cos\varphi(\sigma_{1z} - \sigma_{2z}) + \sin\varphi(\sigma_{1x}\sigma_{2y} - \sigma_{1y}\sigma_{2x})}{4}, \tag{13}$$

and the time evolution under a gradient Zeeman field in z direction, leaving $P_{\uparrow\downarrow}$ and $P_{\uparrow\uparrow}$ invariant and evolves P_S to

$$e^{i\frac{\vartheta}{4}(\sigma_{1z} - \sigma_{2z})} P_S e^{-i\frac{\vartheta}{4}(\sigma_{1z} - \sigma_{2z})} = \frac{\mathbb{1} + \sigma_{1z}\sigma_{2z} + \cos\vartheta(\sigma_{1x}\sigma_{2x} + \sigma_{1y}\sigma_{2y}) + \sin\vartheta(\sigma_{1x}\sigma_{2y} - \sigma_{1y}\sigma_{2x})}{4}. \tag{14}$$

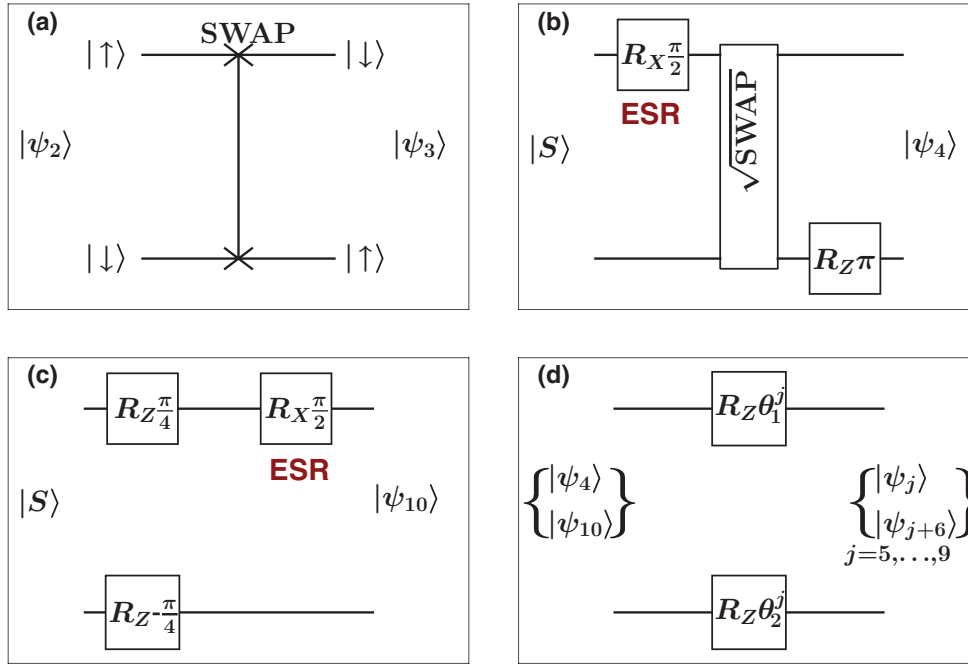


FIG. 2. (Color online) The quantum circuits used to realize the quorum (12). (a) represents the preparation of the state $|\psi_3\rangle$ by a SWAP gate starting from state $|\psi_2\rangle$. The circuits in (b) and (c) show the preparation of the state $|\psi_4\rangle$ and $|\psi_{10}\rangle$, respectively, starting from the singlet state $|S\rangle$. In (d), we show the construction of the remaining states of the quorum, $|\psi_j\rangle$ and $|\psi_{j+6}\rangle$ with $j = 5, \dots, 9$, by rotations R_Z implemented using a static magnetic field, starting from $|\psi_4\rangle$ and $|\psi_{10}\rangle$ respectively. The angles θ_1^j and θ_2^j depend on the index j of the final state but they are the same for the maps $|\psi_4\rangle$ to $|\psi_j\rangle$ and $|\psi_{10}\rangle$ to $|\psi_{j+6}\rangle$. The actual values of θ_1^j and θ_2^j can be found in Eq. (12), e.g., for $j = 9$, they are given by $\theta_1^j = -\theta_2^j = -\pi/2$. Note that ESR is used to implement R_X in the preparation of the states $|\psi_4\rangle$ and $|\psi_{10}\rangle$. The gate $R_X \pi/2$ on the upper line in (b) denotes a rotation of the first qubit around the x axis by the angle $\pi/2$, i.e., the operation $e^{i\frac{\pi}{4}\sigma_{1x}}$. The other rotations R_X and R_Z are defined accordingly.

The single-qubit gates containing σ_{1z} or σ_{2z} can, in principle, be achieved just by waiting for a certain time with negligible J and an applied magnetic field. Since the magnetic field cannot easily be switched off completely this requires precise control of the time which is spent between state preparation and the projective measurement. Considering for example the states $|\psi_4\rangle$ and $|\psi_7\rangle$, we see that the state with spins polarized in x direction, $|\psi_4\rangle$, and the one with both spins in y direction, $|\psi_7\rangle$, are connected just by a rotation around the z axis for both spins, which is realized by a (large) constant magnetic field. But clearly it is necessary to distinguish those states $|\psi_4\rangle$ and $|\psi_7\rangle$ experimentally to get the full information of the density matrix ρ . Therefore state tomography requires more control than would be necessary to demonstrate ESR rotations alone, where the latter could be done by finding experimental evidence for one spin to be flipped by the ESR pulse. For tomography, the relative phase between $|0\rangle$ and $|1\rangle$ needs to be controlled in addition. Note that the adjoint quantum gates included in Eq. (12) are applied on the initial state in the tomography experiment. Afterward a lack of time control might not harm the experiment as a $e^{i\phi(\sigma_{1z}+\sigma_{2z})}$ gate results in no more than a global phase on the states $|\uparrow\downarrow\rangle$, $|\uparrow\uparrow\rangle$, and $|S\rangle$. Only the projection on these states by the spin-to-charge conversion has to be precise. In Appendix D, we give a slightly different realization of the 15 states of Eq. (12). This alternative representation corresponds to a rotating frame.

V. ESTIMATING THE ERROR

Measuring a quantum system always produces statistical results, thus the exact quantum state cannot be determined by an experiment which is performed a finite number of times, but increasing this number of repetitions cannot lead to an arbitrary high accuracy of the estimation for the quantum state either since the measurement scheme unavoidably contains systematic errors. Therefore it is necessary to know how precise the desired measurement scheme is actually performed. We assume the error in the measurement setup to arise mainly from the applied quantum gates, and among those the ESR gate, $e^{i\frac{\pi}{4}\sigma_{1x}}$, to have the largest influence on the total error. In the experiment described in Ref. 4 the exchange was always accompanied by ESR operations, hence the fidelity of exchange alone was not accessible. Errors in the quantum gates may occur due to fluctuations in the magnetic field, for instance, caused by nuclear spins,^{2,39} which is most damaging for the ESR gate. Charge fluctuations mainly influence the exchange interaction and thus the SWAP and $\sqrt{\text{SWAP}}$ gate. Finally, differences in the times for which interactions are actually switched on, affect all quantum gates but in particular the spin rotations around the z axis according to a static magnetic field.

Knowledge about the experimentally realized precision of the projective measurements suggested in Sec. IV, can practically only be gained by prior experiments. One option to

achieve this is a self-consistent tomography^{25,40} where the perfect states from Sec. IV, P_j ($j = 1, \dots, 15$), are replaced by imperfect and unknown ones, P'_j . This implies that before using the set of measurements to determine an unknown quantum state, the set $\{P'_j\}$ itself has to be determined first. For this purpose, one could, e.g., perform measurements to obtain statistical knowledge on the quantities

$$M_{ij} = \text{tr}(P'_i P'_j), \quad i, j = 1, \dots, 15. \quad (15)$$

Note that preparing the system in the state P'_i is the inverted procedure of the projective measurement on this state, starting from a (0,2) charge state. The states P'_j can be determined approximately afterward via a maximum likelihood algorithm^{25,40} up to a basis in Hilbert space that has to be fixed as M_{ij} is invariant under a unitary transformation. Note that here, less information is needed than for quantum process tomography.⁴⁰

Since the 15 states in Sec. IV are generated by a smaller number of different quantum gates, it might be an alternative to describe those gates with a set of parameters including mean fluctuations and determine these parameters experimentally. In general, the imperfect projection operators P'_j would be assumed to depend on a set of n parameters $\alpha_1, \dots, \alpha_n$, for a parameterization of fluctuating magnetic and electric fields see Ref. 25, for a parameter fit of a ESR experiment see Ref. 3. For experiments that are repeated often, we can consider the mixed states $\overline{P'_j}$ calculated from the statistical distribution of the parameters $\alpha_1, \dots, \alpha_n$,

$$\overline{P'_j} = \int d\alpha_1 \dots d\alpha_n p_1(\alpha_1) \dots p_n(\alpha_n) P'_j(\alpha_1, \dots, \alpha_n). \quad (16)$$

For Gaussian distributions, it is sufficient to determine the mean values of α_i and α_i^2 , which means that n^2 numbers have to be extracted from experiments. Note that errors in those values will directly lead to errors in the tomography of an unknown state, but it is not necessary that the distributions are sharp. Nevertheless, the deviations of the mixed states $\overline{P'_j}$ from the pure states P_j worsen the result of the tomography measurement as illustrated by the following example. Assume the matrices $P'_4 - \mathbb{1}/4$ and $P'_6 - \mathbb{1}/4$ to have the same directions in matrix space as $P_4 - \mathbb{1}/4$ and $P_6 - \mathbb{1}/4$, i.e., they are given by

$$P'_j = \frac{1 - f_j^2}{3} \mathbb{1} + \frac{4f_j^2 - 1}{3} P_j, \quad (17)$$

where $f_j = \text{tr}(\sqrt{\overline{P'_j} P'_j} \sqrt{P_j})$ is the fidelity of the quantum state $\overline{P'_j}$ with respect to P_j , and where we assume $f_4 = f_6 = f$ for the remainder of the discussion. For a completely mixed state $P'_j = \mathbb{1}/4$, we find $f = 1/2$. Whereas the parameter ρ_4 from Eq. (4) in the ideal case of projection onto pure states, given by the operators P_4 and P_6 , can be gained by using the equation

$$\rho_4 = \frac{2[\text{tr}(P_4 \rho) + \text{tr}(P_6 \rho)] - 1}{2}, \quad (18)$$

we use another representation of ρ_4 ,

$$\rho_4 = \frac{3\{2[\text{tr}(P'_4 \rho) + \text{tr}(P'_6 \rho)] - 1\}}{2(4f^2 - 1)}, \quad (19)$$

for the projection operators P'_4 and P'_6 , which denotes the projection onto mixed states if $f < 1$. For the statistical error of ρ_4 desired to be smaller than δ , the statistical error of the experimental values for $\text{tr}(P'_4 \rho)$ and $\text{tr}(P'_6 \rho)$, which we assume to be equal, has to be below $\delta' = \frac{(4f^2 - 1)\delta}{3\sqrt{2}}$. A Chernoff bound^{41,42} can be applied to estimate the number of experimental runs needed to realize a desired precision.^{43,44} The possible outcomes of one experimental run are 0 for a (1,1) charge state after the sweep and 1 if a (0,2) charge state is measured, the expectation value is $\text{tr}(P'_j \rho)$. Repeating this experiment N_{run} times thus leads to a binomial distribution. The probability for the experimental value, i.e., the number of runs with result 1 divided by N_{run} , to be out of an interval $[\text{tr}(P'_j \rho) - \delta', \text{tr}(P'_j \rho) + \delta']$, P_{out} , is limited by

$$P_{\text{out}} \leq 2 \exp\left(\frac{-2\delta'^2}{N_{\text{run}}}\right). \quad (20)$$

Therefore the number of experimental runs which provide a P_{out} below a desired limit P_l can be chosen by

$$N_{\text{run}} > \frac{\ln(2/P_l)}{2\delta'^2} = \frac{9 \ln(2/P_l)}{\delta^2(4f^2 - 1)^2}. \quad (21)$$

This means that the reduced fidelity in the projection states can be compensated by increasing the number of experimental repetitions.

VI. CONCLUSION

We have presented a measurement scheme by accessing the states of a quorum for state tomography in the two-qubit space by realistic quantum gates and three types of spin-to-charge conversion in a two-electron double-quantum dot. The quantum gates include SWAP and $\sqrt{\text{SWAP}}$ gates realized by exchange interaction, as well as ESR rotations. We assume the ESR gates to have the largest impact on the fidelity of the quantum states. Therefore it is important that the ESR rotation is applied for no more than a $\pi/2$ rotation per state. Moreover, it should be an advantage that only one of the spins has to be treated with ESR since in the experiment by Brunner and coworkers,⁴ the fidelity of ESR was different for the left and the right quantum dots. Further single-qubit rotations are realized using a static magnetic field requiring precise control of the field tuning and the pulse times.

Whether state tomography can be realized experimentally in the system that we consider here depends on the realization of the different quantum states. A reduced fidelity in the experimental representation of the (pure) quantum states does not prevent the tomographic reconstruction in principle but reduces its quality. The crucial point is the knowledge of the experimenter on which (mixed) states the unknown quantum state is actually projected. A lack of information about this state will in any case limit the precision of the tomography. Self-consistent measurements^{25,40} or a calibration by analyzing the tomography data²⁴ can reduce this lack of knowledge. In general, the accuracy of a realized tomography experiment has to be determined experimentally as well. Our measurement scheme is only one possible solution for state tomography in the two-spin system. The question which scheme is optimal regarding the accuracy of the estimated density matrix with or without a limited number of experimental runs remains

open. The solution will crucially depend on the fidelity of the different quantum gates performed in the system.

ACKNOWLEDGMENTS

We thank Cord A. Müller and András Pályi for useful discussions and the DFG for financial support under the programs SPP 1285 ‘‘Semiconductor spintronics’’ and SFB 767 ‘‘Controlled nanosystems.’’

APPENDIX A: REPRESENTATION OF A PROJECTION ONTO A STATE IN MATRIX SPACE

Assuming that we can perform any unitary operation in our four-level system, we can project on any state

$$|\phi_j\rangle = a_j|\uparrow\uparrow\rangle + b_j|\uparrow\downarrow\rangle + c_j|\downarrow\uparrow\rangle + d_j|\downarrow\downarrow\rangle, \quad (\text{A1})$$

where $|a_j|^2 + |b_j|^2 + |c_j|^2 + |d_j|^2 = 1$, without loss of generality, $a_j \in \mathbb{R}_{\geq 0}$ as a global phase does not matter. The corresponding projector can be written in the matrix form for the basis $\{|\uparrow\uparrow\rangle, |\uparrow\downarrow\rangle, |\downarrow\uparrow\rangle, |\downarrow\downarrow\rangle\}$,

$$P_j = |\phi_j\rangle\langle\phi_j| \equiv \begin{pmatrix} |a_j|^2 & a_j b_j^* & a_j c_j^* & a_j d_j^* \\ b_j a_j^* & |b_j|^2 & b_j c_j^* & b_j d_j^* \\ c_j a_j^* & c_j b_j^* & |c_j|^2 & c_j d_j^* \\ d_j a_j^* & d_j b_j^* & d_j c_j^* & |d_j|^2 \end{pmatrix} \\ = \sum_{i,l=0,x,y,z} n_{jil} \frac{\sigma_{1i}\sigma_{2l}}{2} \quad (\text{A2})$$

with

$$n_{j00} = \frac{|a_j|^2 + |b_j|^2 + |c_j|^2 + |d_j|^2}{2} = \frac{1}{2}, \\ n_{j0x} = \frac{a_j^* b_j + b_j^* a_j + c_j^* d_j + d_j^* c_j}{2}, \\ n_{j0y} = \frac{a_j^* b_j - b_j^* a_j + c_j^* d_j - d_j^* c_j}{2i}, \\ n_{j0z} = \frac{|a_j|^2 - |b_j|^2 + |c_j|^2 - |d_j|^2}{2},$$

$$\left\langle P_j - \frac{\mathbb{1}}{4} \middle| P_i - \frac{\mathbb{1}}{4} \right\rangle_M = 0 \Leftrightarrow \langle P_j | P_i \rangle_M = \frac{1}{4} \Leftrightarrow |\langle\phi_j|\phi_i\rangle|^2 = \frac{1}{4}, \quad (\text{B1})$$

which means that the traceless parts of the projection operators P_j would be orthogonal with respect to $\langle\cdot|\cdot\rangle_M$. Analogously, for a single spin, the density matrix can be determined by projections on the x , y , and z axes of the corresponding Bloch sphere. However, for our four-level system, Eq. (B1) cannot be fulfilled for 15 projection operators of the form $P_j = |\phi_j\rangle\langle\phi_j|$, which we show in this appendix. For the proof, we use the following lemma.

Lemma. Let V_1 and V_2 be two real Euclidean spaces with dimension n_1 and n_2 . Let $\{a_1, \dots, a_{n_1+n_2}\}$ be an orthogonal basis in the space $V_1 \oplus V_2$ with $|a_j|^2 = c > 0$, $|P_{V_1} a_j|^2 = c_1$, and $|P_{V_2} a_j|^2 = c_2 \forall j = 1, \dots, n_1 + n_2$, where P_{V_1} (P_{V_2}) is the projection on the space V_1 (V_2). Then c_1 and c_2 fulfill

$$\frac{c_1}{c_2} = \frac{n_1}{n_2}. \quad (\text{B2})$$

$$n_{jx0} = \frac{a_j^* c_j + b_j^* d_j + c_j^* a_j + d_j^* b_j}{2}, \\ n_{jxx} = \frac{a_j^* d_j + d_j^* a_j + b_j^* c_j + c_j^* b_j}{2}, \\ n_{jxy} = \frac{a_j^* d_j - d_j^* a_j - b_j^* c_j + c_j^* b_j}{2i}, \\ n_{jxz} = \frac{a_j^* c_j - b_j^* d_j + c_j^* a_j - d_j^* b_j}{2}, \\ n_{jy0} = \frac{a_j^* c_j + b_j^* d_j - c_j^* a_j - d_j^* b_j}{2i}, \\ n_{jyx} = \frac{a_j^* d_j - d_j^* a_j + b_j^* c_j - c_j^* b_j}{2i}, \\ n_{jyy} = \frac{b_j^* c_j + c_j^* b_j - a_j^* d_j - d_j^* a_j}{2}, \\ n_{jyz} = \frac{a_j^* c_j - b_j^* d_j - c_j^* a_j + d_j^* b_j}{2i}, \\ n_{jz0} = \frac{|a_j|^2 + |b_j|^2 - |c_j|^2 - |d_j|^2}{2}, \\ n_{jzx} = \frac{a_j^* b_j + b_j^* a_j - c_j^* d_j - d_j^* c_j}{2}, \\ n_{jzy} = \frac{a_j^* b_j - b_j^* a_j - c_j^* d_j + d_j^* c_j}{2i}, \\ n_{jzz} = \frac{|a_j|^2 - |b_j|^2 - |c_j|^2 + |d_j|^2}{2}. \quad (\text{A3})$$

APPENDIX B: NO ORTHOGONAL BASIS IN TRACELESS MATRIX SPACE BY PROJECTORS ON SINGLE PURE STATES

For the reconstruction of the density matrix from the measurement data, it would be ideal to have a set $\{P_1, \dots, P_{15}\}$, which fulfills, for $i \neq j$,

Proof. We denote $a_1, \dots, a_{n_1+n_2}$ in an orthonormal basis $\{e_1, \dots, e_{n_1}, e_{n_1+1}, \dots, e_{n_1+n_2}\}$ where the vectors e_1, \dots, e_{n_1} are completely in V_1 and $e_{n_1+1}, \dots, e_{n_1+n_2}$ are completely in V_2 . Now, we can write the normalized vectors $a_1/\sqrt{c}, \dots, a_{n_1+n_2}/\sqrt{c}$ as the columns of a matrix A with the matrix elements $A_{ij} = \langle e_i | a_j \rangle / \sqrt{c}$. The matrix A is an orthogonal matrix, i.e., it fulfills $A^T A = \mathbb{1}$ but also $AA^T = \mathbb{1}$, which reflects the fact that rows and columns denote orthonormal bases in $V_1 \oplus V_2$. From the conditions in the lemma, we find

$$\sum_{i=1}^{n_1} A_{ij}^2 = \frac{c_1}{c} \quad \text{and} \quad \sum_{i=n_1+1}^{n_1+n_2} A_{ij}^2 = \frac{c_2}{c}, \quad (\text{B3})$$

and thus

$$\sum_{j=1}^{n_1+n_2} \sum_{i=1}^{n_1} A_{ij}^2 = (n_1 + n_2) \frac{c_1}{c} \quad (\text{B4})$$

and

$$\sum_{j=1}^{n_1+n_2} \sum_{i=n_1+1}^{n_1+n_2} A_{ij}^2 = (n_1 + n_2) \frac{c_2}{c}.$$

On the other hand, using that the rows of A denote orthonormal vectors in $\mathbb{R}^{n_1+n_2}$ yields

$$\sum_{i=1}^{n_1} \sum_{j=1}^{n_1+n_2} A_{ij}^2 = \sum_{i=1}^{n_1} 1 = n_1 \quad (\text{B5})$$

and

$$\sum_{i=n_1+1}^{n_1+n_2} \sum_{j=1}^{n_1+n_2} A_{ij}^2 = \sum_{i=n_1+1}^{n_1+n_2} 1 = n_2.$$

Building the ratio directly leads to

$$\frac{\sum_{j=1}^{n_1+n_2} \sum_{i=1}^{n_1} A_{ij}^2}{\sum_{j=1}^{n_1+n_2} \sum_{i=n_1+1}^{n_1+n_2} A_{ij}^2} \stackrel{(\text{B4})}{=} \frac{c_1}{c_2} \stackrel{(\text{B5})}{=} \frac{n_1}{n_2}. \quad (\text{B6})$$

Now we come back to the 15 basis states for the space of traceless Hermitian matrices constructed by pure states in four-dimensional Hilbert space. We use the notation from Appendix A. Assume that $|\phi_1\rangle = |\uparrow\uparrow\rangle$, if it is not, we can perform a unitary transformation to match this starting point. The corresponding projector is $P_1 = (\mathbb{1} + \sigma_{1z} + \sigma_{2z} + \sigma_{1z}\sigma_{2z})/4$. It follows that $a_j = 1/2$ in order to fulfill $|\langle\phi_1|\phi_j\rangle|^2 = 1/4$ for $j = 2, \dots, 15$. Therefore we get

$$\begin{aligned} n_{j00} &= \frac{1}{2}, \\ n_{j0x} &= \frac{\text{Re } b_j + c_j^* d_j + d_j^* c_j}{2}, \\ n_{j0y} &= \frac{\text{Im } b_j + c_j^* d_j - d_j^* c_j}{2i}, \\ n_{j0z} &= \frac{\frac{1}{4} - |b_j|^2 + |c_j|^2 - |d_j|^2}{2}, \\ n_{jx0} &= \frac{\text{Re } c_j + b_j^* d_j + d_j^* b_j}{2}, \\ n_{jxx} &= \frac{\text{Re } d_j + b_j^* c_j + c_j^* b_j}{2}, \\ n_{jxy} &= \frac{\text{Im } d_j - b_j^* c_j + c_j^* b_j}{2i}, \\ n_{jxz} &= \frac{\text{Re } c_j - b_j^* d_j - d_j^* b_j}{2}, \\ n_{jy0} &= \frac{\text{Im } c_j + b_j^* d_j - d_j^* b_j}{2i}, \\ n_{jyx} &= \frac{\text{Im } d_j + b_j^* c_j - c_j^* b_j}{2i}, \\ n_{jyy} &= \frac{b_j^* c_j + c_j^* b_j - \text{Re } d_j}{2}, \\ n_{jyz} &= \frac{\text{Im } c_j - b_j^* d_j + d_j^* b_j}{2i}, \\ n_{jz0} &= \frac{\frac{1}{4} + |b_j|^2 - |c_j|^2 - |d_j|^2}{2}, \end{aligned} \quad (\text{B7})$$

$$\begin{aligned} n_{jzx} &= \frac{\text{Re } b_j - c_j^* d_j - d_j^* c_j}{2}, \\ n_{jzy} &= \frac{\text{Im } b_j - c_j^* d_j + d_j^* c_j}{2i}, \\ n_{jzz} &= \frac{\frac{1}{4} - |b_j|^2 - |c_j|^2 + |d_j|^2}{2}. \end{aligned}$$

Now we define a new basis of the space of 4×4 matrices, $\{\tau_i; i = 0, \dots, 15\}$ with

$$\begin{aligned} \tau_0 &= \frac{\mathbb{1}}{2}, \quad \tau_1 = \frac{\sigma_{2z} + \sigma_{1z} + \sigma_{1z}\sigma_{2z}}{2\sqrt{3}}, \\ \tau_2 &= \frac{\sigma_{1x} + \sigma_{1x}\sigma_{2z}}{2\sqrt{2}}, \quad \tau_3 = \frac{\sigma_{2x} + \sigma_{1z}\sigma_{2x}}{2\sqrt{2}}, \\ \tau_4 &= \frac{\sigma_{1y} + \sigma_{1y}\sigma_{2z}}{2\sqrt{2}}, \quad \tau_5 = \frac{\sigma_{2y} + \sigma_{1z}\sigma_{2y}}{2\sqrt{2}}, \\ \tau_6 &= \frac{\sigma_{1x}\sigma_{2x} - \sigma_{1y}\sigma_{2y}}{2\sqrt{2}}, \quad \tau_7 = \frac{\sigma_{1x}\sigma_{2y} + \sigma_{1y}\sigma_{2x}}{2\sqrt{2}}, \\ \tau_8 &= \frac{\sigma_{1x} - \sigma_{1x}\sigma_{2z}}{2\sqrt{2}}, \quad \tau_9 = \frac{\sigma_{2x} - \sigma_{1z}\sigma_{2x}}{2\sqrt{2}}, \\ \tau_{10} &= \frac{\sigma_{1y} - \sigma_{1y}\sigma_{2z}}{2\sqrt{2}}, \quad \tau_{11} = \frac{\sigma_{2y} - \sigma_{1z}\sigma_{2y}}{2\sqrt{2}}, \\ \tau_{12} &= \frac{\sigma_{1x}\sigma_{2x} + \sigma_{1y}\sigma_{2y}}{2\sqrt{2}}, \quad \tau_{13} = \frac{\sigma_{1x}\sigma_{2y} - \sigma_{1y}\sigma_{2x}}{2\sqrt{2}}, \\ \tau_{14} &= \frac{\sigma_{1z} - \sigma_{2z}}{2\sqrt{2}}, \quad \tau_{15} = \frac{\sigma_{1z} + \sigma_{2z} - 2\sigma_{1z}\sigma_{2z}}{2\sqrt{6}}, \end{aligned} \quad (\text{B8})$$

which again fulfills $\langle\tau_k|\tau_l\rangle_M = \delta_{kl}$. $P_2 - \mathbb{1}/4, \dots, P_{15} - \mathbb{1}/4$ are now supposed to be an orthogonal basis in the space spanned by τ_2, \dots, τ_{15} . We show that this is not possible for the following reason. When we expand P_j in the new basis, $P_j = \sum_i m_{ji} \tau_i$, we find easily for $j \geq 2$ from Eq. (B7) that

$$\begin{aligned} m_{j0} &= \frac{1}{2}, \quad m_{j1} = 0, \\ m_{j2} &= \frac{\text{Re } c_j}{\sqrt{2}}, \quad m_{j3} = \frac{\text{Re } b_j}{\sqrt{2}}, \quad m_{j4} = \frac{\text{Im } c_j}{\sqrt{2}}, \\ m_{j5} &= \frac{\text{Im } b_j}{\sqrt{2}}, \quad m_{j6} = \frac{\text{Re } d_j}{\sqrt{2}}, \quad m_{j7} = \frac{\text{Im } d_j}{\sqrt{2}}, \end{aligned} \quad (\text{B9})$$

and thus

$$\sum_{i=2}^7 m_{ji}^2 = \frac{|b_j|^2 + |c_j|^2 + |d_j|^2}{2} = \frac{1 - |a_j|^2}{2} = \frac{3}{8}. \quad (\text{B10})$$

On the other hand, due to $\text{tr}(P_j) = 1$ and $P_j^2 = P_j$, we find for $j = 2, \dots, 15$,

$$\begin{aligned} 1 &= \langle P_j | P_j \rangle_M = \sum_{i=0}^{15} m_{ji}^2 = m_{j0}^2 + m_{j1}^2 + \sum_{i=2}^{15} m_{ji}^2 \\ &= \frac{1}{4} + \sum_{i=2}^{15} m_{ji}^2, \end{aligned} \quad (\text{B11})$$

which yields

$$\sum_{i=2}^{15} m_{ji}^2 = \frac{3}{4}. \quad (\text{B12})$$

Using Eq. (B10), we find

$$\sum_{i=8}^{15} m_{ji}^2 = \frac{3}{4} - \sum_{i=2}^7 m_{ji}^2 = \frac{3}{8} \quad (\text{B13})$$

and thus

$$\frac{\sum_{i=2}^7 m_{ji}^2}{\sum_{i=8}^{15} m_{ji}^2} = 1 \neq \frac{6}{8}, \quad (\text{B14})$$

which means that the ratio of the projections of P_j on the subspace $\text{span}\{\tau_2, \dots, \tau_7\}$ and $\text{span}\{\tau_8, \dots, \tau_{15}\}$ is a fixed value that does not correspond to the dimensions of these subspaces and thus violates the lemma above. Therefore an orthogonal basis for $\text{span}\{\tau_1, \dots, \tau_{15}\}$ cannot be constructed by $P_1 - \mathbb{1}/4, \dots, P_{15} - \mathbb{1}/4$.

APPENDIX C: RECONSTRUCTION WITH MUTUALLY UNBIASED BASES

Here, we show that $|\det(\mathcal{P})| = \frac{1}{32}$ if the matrix \mathcal{P} as introduced in Sec. III is gained from five mutually unbiased bases, including three states from each basis, $\{|\phi_{01}\rangle, |\phi_{02}\rangle, |\phi_{03}\rangle, |\phi_{11}\rangle, \dots, |\phi_{43}\rangle\}$. The rows of \mathcal{P} represents the traceless parts of the corresponding projection operators $P_{3j+k} = |\phi_{jk}\rangle\langle\phi_{jk}|$, which we denote

$$\mathcal{P}_l = ((P_l|D_1)_M, \dots, (P_l|D_{15})_M). \quad (\text{C1})$$

We want to apply Gram-Schmidt orthogonalization on the row vectors \mathcal{P}_l that leaves the determinant of \mathcal{P} invariant. As

$$\mathcal{P}_{3j+k} \mathcal{P}_{3i+l}^T = |\langle\phi_{jk}|\phi_{il}\rangle|^2 - \frac{1}{4} = \delta_{ij} (\delta_{kl} - \frac{1}{4})$$

with $i, j \in \{1, \dots, 5\}$ and $k, l \in \{1, 2, 3\}$, (C2)

we only have to orthogonalize the five three-dimensional subspaces for $i = j$. From $\mathcal{P}_{3j+k} \mathcal{P}_{3j+l}^T = \delta_{kl} - \frac{1}{4}$, we gain easily the orthogonalized row vectors from the Gram-Schmidt method,

$$\begin{aligned} \mathcal{P}'_{3j+1} &= \mathcal{P}_{3j+1}, \\ \mathcal{P}'_{3j+2} &= \mathcal{P}_{3j+2} + \frac{1}{3} \mathcal{P}_{3j+1}, \\ \mathcal{P}'_{3j+3} &= \mathcal{P}_{3j+3} + \frac{1}{2} \mathcal{P}'_{3j+2} + \frac{1}{3} \mathcal{P}_{3j+1}, \end{aligned} \quad (\text{C3})$$

which have the lengths $\sqrt{\frac{3}{4}}$, $\sqrt{\frac{2}{3}}$, and $\sqrt{\frac{1}{2}}$. A unitary transformation does not change the determinant and transforms \mathcal{P}' to a diagonal matrix. Therefore we find

$$\det(\mathcal{P}) = \det(\mathcal{P}') = \left(\sqrt{\frac{3}{4}} \sqrt{\frac{2}{3}} \sqrt{\frac{1}{2}} \right)^5 = \left(\frac{1}{2} \right)^5 = \frac{1}{32}. \quad (\text{C4})$$

APPENDIX D: REALIZATION OF THE TOMOGRAPHY SCHEME IN THE ROTATING FRAME

In this appendix, we present a modified realization of the 15 states of Eq. (12),

$$\begin{aligned} |\psi_1\rangle &= |\uparrow\uparrow\rangle, \\ |\psi_2\rangle &= |\uparrow\downarrow\rangle, \\ |\psi_3\rangle &= \text{SWAP} |\uparrow\downarrow\rangle, \\ |\psi_4\rangle &= e^{i\frac{\pi}{2}\sigma_{2z}} \sqrt{\text{SWAP}} e^{i\frac{\pi}{4}\sigma_{1x}} |S\rangle, \\ |\psi_5\rangle &= \sqrt{\text{SWAP}} e^{-i\frac{\pi}{4}\sigma_{1x}} |S\rangle, \\ |\psi_6\rangle &= e^{i\frac{\pi}{2}\sigma_{2z}} |\psi_4\rangle, \\ |\psi_7\rangle &= e^{i\frac{\pi}{2}\sigma_{2z}} \sqrt{\text{SWAP}} e^{i\frac{\pi}{4}\sigma_{1y}} |S\rangle, \\ |\psi_8\rangle &= \sqrt{\text{SWAP}} e^{-i\frac{\pi}{4}\sigma_{1y}} |S\rangle, \\ |\psi_9\rangle &= e^{i\frac{\pi}{2}\sigma_{2z}} |\psi_7\rangle, \\ |\psi_{10}\rangle &= e^{-i\frac{\pi}{4}\sigma_{2z}} e^{i\frac{\pi}{4}\sigma_{1x}} |S\rangle, \\ |\psi_{11}\rangle &= e^{i\frac{\pi}{4}\sigma_{2z}} e^{-i\frac{\pi}{4}\sigma_{1x}} |S\rangle, \\ |\psi_{12}\rangle &= e^{i\frac{\pi}{2}\sigma_{2z}} |\psi_{10}\rangle, \\ |\psi_{13}\rangle &= e^{-i\frac{\pi}{4}\sigma_{2z}} e^{i\frac{\pi}{4}\sigma_{1y}} |S\rangle, \\ |\psi_{14}\rangle &= e^{-i\frac{3\pi}{4}\sigma_{2z}} e^{-i\frac{\pi}{4}\sigma_{1y}} |\psi_{13}\rangle, \\ |\psi_{15}\rangle &= e^{i\frac{\pi}{2}\sigma_{2z}} |\psi_{13}\rangle. \end{aligned} \quad (\text{D1})$$

Here, the local quantum gates contain only σ_{1x} , σ_{1y} , and σ_{2z} . Therefore this representation corresponds to a rotating frame of reference where the rotation axis is the z axis and the frequency is given by the Zeeman splitting in the first dot, $2h_{1z}$. The gates $e^{i\theta\sigma_{2z}}$ occur within the rotating frame due to the difference in the Zeeman energies in dots 1 and 2, thus $\theta = (h_{2z} - h_{1z})t = -\Delta h_z t$ holds for a time interval t . This rotation of the second qubit occurs slowly in the rotating frame, because the difference in the Zeeman splittings, $|\Delta h_z|$, is typically much smaller than $|h_{2z}|$. The gates $e^{i\frac{\pi}{4}\sigma_{1x}}$, $e^{-i\frac{\pi}{4}\sigma_{1x}}$, $e^{i\frac{\pi}{4}\sigma_{1y}}$, and $e^{-i\frac{\pi}{4}\sigma_{1y}}$ are realized by applying ESR pulses, $H_{\text{ESR}} = h_{1z}\sigma_z + h_{1x} \cos(2h_{1z}t + \phi_{\text{shift}})\sigma_x$, which leads in the rotating frame to the gate $\exp[ih_{1x}t/2(\cos\phi_{\text{shift}}\sigma_{1x} + \sin\phi_{\text{shift}}\sigma_{1y})]$. Hence the phase ϕ_{shift} has to be chosen 0, π , $\pi/2$, or $3\pi/2$, respectively. The statement that we need at most $\pi/2$ ESR rotations in only one dot per measurement still holds in the new realization (D1). The timing condition for the rotation around the z axis, which we face in the laboratory frame is shifted to the control of the phase ϕ_{shift} in the rotating frame. Note that the quantum gates applied in Eqs. (12) and (D1) are not all identical but the states $|\psi_1\rangle, \dots, |\psi_{15}\rangle$ are the same up to irrelevant global phases.

¹D. Loss and D. P. DiVincenzo, *Phys. Rev. A* **57**, 120 (1998).

²J. R. Petta, A. C. Johnson, J. M. Taylor, E. A. Laird, A. Yacoby, M. D. Lukin, C. M. Marcus, M. P. Hanson, and A. C. Gossard, *Science* **309**, 2180 (2005).

³F. H. L. Koppens, C. Buizert, K. J. Tielrooij, I. T. Vink, K. C. Nowack, T. Meunier, L. P. Kouwenhoven, and L. M. K. Vandersypen, *Nature (London)* **442**, 766 (2006).

⁴R. Brunner, Y.-S. Shin, T. Obata, M. Pioro-Ladrière, T. Kubo, K. Yoshida, T. Taniyama, Y. Tokura, and S. Tarucha, *Phys. Rev. Lett.* **107**, 146801 (2011).

⁵M. D. de Burgh, N. K. Langford, A. C. Doherty, and A. Gilchrist, *Phys. Rev. A* **78**, 052122 (2008).

⁶Z. Hradil, *Phys. Rev. A* **55**, R1561 (1997).

⁷D. F. V. James, P. G. Kwiat, W. J. Munro, and A. G. White, *Phys. Rev. A* **64**, 052312 (2001).

- ⁸J. A. Smolin, J. M. Gambetta, and G. Smith, *Phys. Rev. Lett.* **108**, 070502 (2012).
- ⁹C. W. Helstrom, *J. Stat. Phys.* **1**, 231 (1969).
- ¹⁰F. Tanaka and F. Komaki, *Phys. Rev. A* **71**, 052323 (2005).
- ¹¹K. R. W. Jones, *Ann. Phys.* **207**, 140 (1991).
- ¹²R. Derka, V. Bužek, G. Adam, and P. L. Knight, *Fine Mech. Opt.* **11/12**, 341 (1996).
- ¹³R. Derka, V. Bužek, and G. Adam, *Acta Physica Slovaca* **46**, 355 (1996).
- ¹⁴V. Bužek, R. Derka, G. Adam, and P. L. Knight, *Ann. Phys.* **266**, 454 (1998).
- ¹⁵R. Schack, T. A. Brun, and C. M. Caves, *Phys. Rev. A* **64**, 014305 (2001).
- ¹⁶R. Blume-Kohout, *New J. Phys.* **12**, 043034 (2010).
- ¹⁷I. L. Chuang, N. Gershenfeld, and M. Kubinec, *Phys. Rev. Lett.* **80**, 3408 (1998).
- ¹⁸C. F. Roos, G. P. T. Lancaster, M. Riebe, H. Häffner, W. Hänsel, S. Gulde, C. Becher, J. Eschner, F. Schmidt-Kaler, and R. Blatt, *Phys. Rev. Lett.* **92**, 220402 (2004).
- ¹⁹H. Häffner, C. F. Roos, and R. Blatt, *Phys. Rep.* **469**, 155 (2008).
- ²⁰H. Häffner, W. Hänsel, C. F. Roos, J. Benhelm, D. Chek-al-kar, M. Chwalla, T. Körber, U. D. Rapol, M. Riebe, P. O. Schmidt *et al.*, *Nature (London)* **438**, 643 (2005).
- ²¹M. Steffen, M. Ansmann, R. McDermott, N. Katz, R. C. Bialczak, E. Lucero, M. Neeley, E. M. Weig, A. N. Cleland, and J. M. Martinis, *Phys. Rev. Lett.* **97**, 050502 (2006).
- ²²M. Steffen, M. Ansmann, R. C. Bialczak, N. Katz, E. Lucero, R. McDermott, M. Neeley, E. M. Weig, A. N. Cleland, and J. M. Martinis, *Science* **313**, 1423 (2006).
- ²³S. Foletti, H. Bluhm, D. Mahalu, V. Umansky, and A. Yacoby, *Nat. Phys.* **5**, 903 (2009).
- ²⁴M. D. Shulman, O. E. Dial, S. P. Harvey, H. Bluhm, V. Umansky, and A. Yacoby, *Science* **336**, 202 (2012).
- ²⁵J. Medford, J. Beil, J. M. Taylor, S. D. Bartlett, A. C. Doherty, E. I. Rashba, D. P. DiVincenzo, H. Lu, A. C. Gossard, and C. M. Marcus, arXiv:1302.1933.
- ²⁶I. D. Ivanović, *J. Phys. A: Math. Gen.* **14**, 3241 (1981).
- ²⁷W. K. Wootters and B. D. Fields, *Ann. Phys.* **191**, 363 (1989).
- ²⁸A. Klappenecker and M. Rötteler, in *Finite Fields and Applications*, edited by G. L. Mullen, A. Poli, and H. Stichtenoth, Lecture Notes in Computer Science, Vol. 2948 (Springer, Berlin, Heidelberg, 2004), p. 137.
- ²⁹T. Durt, B.-G. Englert, I. Bengtsson, and K. Życzkowski, *Int. J. Quantum Inf.* **8**, 535 (2010).
- ³⁰C. Kloeffel and D. Loss, *Ann. Rev. Condens. Matt. Phys.* **4**, 51 (2013).
- ³¹M. Pioro-Ladrière, T. Obata, Y. Tokura, Y.-S. Shin, T. Kubo, K. Yoshida, T. Taniyama, and S. Tarucha, *Nat. Phys.* **4**, 776 (2008).
- ³²S. Nadj-Perge, S. M. Frolov, E. P. A. M. Bakkers, and L. P. Kouwenhoven, *Nature (London)* **468**, 1084 (2010).
- ³³K. P. Petersson, L. W. McFaul, M. D. Schroer, M. Jung, J. M. Taylor, A. A. Houck, and J. R. Petta, *Nature (London)* **490**, 380 (2012).
- ³⁴G. Burkard and A. Imamoglu, *Phys. Rev. B* **74**, 041307 (2006).
- ³⁵B. E. Kane, *Nature (London)* **393**, 133 (1998).
- ³⁶L. M. K. Vandersypen, R. Hanson, L. H. W. van Beveren, J. M. Elzerman, J. S. Greidanus, S. D. Franceschi, and L. P. Kouwenhoven, in *Quantum Computing and Quantum Bits in Mesoscopic Systems*, edited by A. Leggett, B. Ruggiero, and P. Silvestrini (Kluwer Academic/Plenum, New York, 2004), p. 201.
- ³⁷H. Ribeiro and G. Burkard, *Phys. Rev. Lett.* **102**, 216802 (2009).
- ³⁸H. Ribeiro, J. R. Petta, and G. Burkard, *Phys. Rev. B* **82**, 115445 (2010).
- ³⁹A. V. Khaetskii, D. Loss, and L. Glazman, *Phys. Rev. Lett.* **88**, 186802 (2002).
- ⁴⁰S. T. Merkel, J. M. Gambetta, J. A. Smolin, S. Poletto, A. D. Córcoles, B. R. Johnson, C. A. Ryan, and M. Steffen, arXiv:1211.0322.
- ⁴¹H. Chernoff, *Ann. Math. Statist.* **23**, 493 (1952).
- ⁴²W. Hoeffding, *J. Am. Stat. Assoc.* **58**, 13 (1963).
- ⁴³A. Bendersky, F. Pastawski, and J. P. Paz, *Phys. Rev. Lett.* **100**, 190403 (2008).
- ⁴⁴A. Bendersky and J. P. Paz, *Phys. Rev. A* **87**, 012122 (2013).
- ⁴⁵Note that a state in a four-dimensional Hilbert space is given by four complex, i.e., eight real parameters, but two of them are fixed here due to normalization and the irrelevance of a global phase.